UnderSCORE: A proof-of-concept understorey Decision Support System (DSS)
Technical manual

Authors: Haben Blondeel[1]**,** Dries Landuyt[1], Michael P. Perring[,1,2, †] and Kris Verheyen[1]

Correspondence to: haben.blondeel@ugent.be

Addresses:

[1]: Forest & Nature Lab, Department of Environment, Ghent University, Campus Gontrode, Geraardsbergsesteenweg 267, 9090 Melle-Gontrode, BELGIUM

[2]: Ecosystem Restoration and Intervention Ecology Research Group, School of Biological Sciences, The University of Western Australia, 35 Stirling Highway, Crawley, WA 6009 AUSTRALIA

† Current: UKCEH, Deiniol Road, Bangor, Gwynedd LL57 2UW, UNITED KINGDOM

Abstract

Numerous decision-makers have an interest in how forest biodiversity and functioning will alter under environmental change. Currently, forest management models focus predominantly on trees and ignore the herbaceous layer (the understorey). This is a crucial oversight, as the understorey is a biodiversity reservoir, provides vital ecosystem services and can influence forest functioning. We investigated whether decision-makers in forest management across Europe consider the understorey when facing uncertainty. We distributed a questionnaire to decision-makers to assess what objectives drive management decisions. Biodiversity loss, forest regeneration and climate change were top priorities, motivated by a sense of environmental protection. Respondents identified the understorey as an "Important" target and infrequently used recognized decision support systems (DSS). We reviewed available forest management DSS and found a lack of understorey-oriented DSS. We subsequently designed a prototype of an understorey DSS to aid decision-makers in their quest to attain biodiverse and resilient forests for the future. The methods and technicalities of this working prototype of "UnderSCORE" are explained in this report.

1 Introduction

1.1 Project outline

The ERC proof-of-concept project UnderSCORE (2020) is a proof-of-concept web-based Decision Support System (DSS) to score forest understorey dynamics in response to management interventions in a changing world. One tool for decision-making (in general, and in forest management in particular) is the use of predictive decision support systems (DSS). Decision support systems have varied conceptualizations (Gordon et al., 2014), but can be an integrated system to provide support around decision problems, by combining a user interface, simulation tool, expert rules, stakeholder preferences, database management and optimization algorithms (Muys et al., 2010).

Currently, forest management models focus predominantly on tree dynamics following interventions (Landuyt et al., 2018), and tend to ignore the plant species found below the trees on the forest floor (below ca. 1 m the understorey). Ignoring the understorey is a crucial oversight, as this vegetation is the major component of floral biodiversity; provides vital ecosystem services (properties that ensure human wellbeing: e.g. food supply, pollinator habitat and resources, recreational visits for wildflowers); and, can influence the overall functioning of the forest with its impact on – for instance - nutrient cycling and forest regeneration (Gilliam, 2007; Landuyt et al., 2019). A greater emphasis from policy makers and society on maintaining and enhancing biodiversity values of forests requires managers and auditors to be aware of likely outcomes of management interventions for the understorey. However, there is a general ignorance of such outcomes. As such, there is a need for a user-friendly tool to help predict key understorey characteristics (e.g. biodiversity, share of species of conservation concern) across environmental contexts and overstorey tree management. The construction of a user-friendly tool requires an underlying model that can predict forest understorey dynamics in relation to environmental and management contexts.

Preceding the development of the proof of concept DSS described herein, we performed a study on the availability and needs for an understorey DSS. We investigated the availability of an understorey component in existing DSS through a literature review, combined with a questionnaire on the need for such a DSS to support decision-makers in forest management (Blondeel et al., 2021). We honed in on the availability of, and requirements for, understorey DSS in a European context, targeted towards decision-makers active in (mixed) temperate forest. We found that regardless of specific occupation (forest manager, policy maker, scientist, consultant, educator), respondents focused on mitigating and adapting to climate change, sustaining forest regeneration, and preventing biodiversity loss, strongly motivated by a sense of environmental protection. These foci require a consideration of the

understorey, given its importance as a biodiversity reservoir, for tree regeneration, and as an indicator to forest responses to climate change.

We aimed to fill the void in understorey-oriented DSS by developing a working prototype of a web-based DSS (UnderSCORE), to support decision-makers when facing uncertainty in forest conservation and management in a changing world. The name "UnderSCORE" emphasizes (underscores) the requirement to consider the overlooked understorey, and reflects its output: easily comprehended scores for different understorey indicators which users can compare across environmental and management contexts and over time. This tool transfers the research output of the [ERC PASTFORWARD](#) project (2015 – 2019) into a shape that is of direct use for policy makers and forest managers. Such a tool is not currently available but clear legal and societal imperatives (e.g. Natura 2000, European Biodiversity Strategy) require its development, and provide the context for its adoption by potential users.

UnderSCORE is, simply put, a practical application of the findings from the research in the PASTFORWARD project, by assessing the need for decision support on understorey management. The focus of understorey change due to multiple environmental changes and management are the shared benchmarks between UnderSCORE and PASTFORWARD. However, as the name suggests, PASTFORWARD had a specific focus of accounting for past dynamics, and those of land-use legacies in particular. Given the proof-of-concept nature of UnderSCORE, we specifically decided to exclude any land-use transitions into the predictions, by focusing only on ancient forest (sites continuously forested since at least 1850). UnderSCORE intends to include such past dynamics in its predictions in future versions that would build on this prototype. The current prototype of the tool focuses on the combined effects of multiple environmental changes (climate warming, atmospheric N deposition, and canopy change) on four selected understorey characteristics (richness, cover, proportion of woody species, and proportion of forest specialists).

1.2   Scope of the UnderSCORE DSS

Ecosystems are globally threatened by multiple environmental change drivers that have joint effects on ecosystem patterns and processes (Bowler et al., 2020). For temperate understorey vegetation in Europe, among the key drivers are climate change, atmospheric nitrogen (N) deposition, and forest canopy change due to management (Bernhardt-Römermann et al., 2015; Landuyt et al., 2019, 2018). Climate change can induce a "thermophilization" of the understorey, due to an insurgence of warm-loving plants at the expense of cold-loving plants (De Frenne et al., 2013; Zellweger et al., 2020). Excess atmospheric N deposition can cause acidification and eutrophication (N saturation) at the forest floor (Bobbink et al., 2010; De Schrijver et al., 2011; Schmitz et al., 2019), with potential species loss due to an increasing insurgence of generalist nutrient-loving plants at the expense of less nutrient demanding

plants (Staude et al., 2020; Verheyen et al., 2012). These effects can be accelerated when canopies are opened due to e.g. the removal of trees in forest management (Verheyen et al., 2012; Zellweger et al., 2020), as light can accelerate plant responses to warming (Blondeel et al., 2020; De Frenne et al., 2015) and eutrophication (DeMalach et al., 2017; Hautier et al., 2009). The joint effects of these three environmental changes can act in unison, and may produce counter-intuitive combined effects due to non-linear relationships between the environmental variables (De Laender, 2018).

UnderSCORE predicts four understorey properties: species richness, cover (%), proportion of woody species (%) and proportion of forest specialists (%). Richness is a simple measure of the number of species. Understorey cover is a simple measure to assess productivity. Compositional change is assessed via the relative amount of woody species (which includes tree regeneration) and the relative amount of typical forest species (which is of conservation concern). UnderSCORE provides trends in these understorey properties in scenarios of environmental change for the period of 2020-2050.

This working prototype of UnderSCORE is built on a frequentist statistical-based model using GAM (general additive models) to predict the mean values of understorey properties in temperate Europe. This prototype operates with formulated scenarios provided by the IPCC and European Union. The UnderSCORE DSS can account for average environmental conditions in EU regions, for the focal environmental variables (mean annual temperature, N deposition), but also for soil conditions (pH) and precipitation (mean annual precipitation) in the regions (Table 1).

Table 1. Schematic overview of the UnderSCORE DSS scope

UNDERSCORE…	
✓ DOES	✘ Does NOT
✓ Use average environmental conditions of the EU regions	✘ Use fine-scale local environmental conditions
✓ Use fixed climate change and N deposition scenarios	✘ Use dynamic climate change and N deposition scenarios with feed-backs
✓ Use a statistical approach	✘ Use a mechanistic approach
✓ Predict based on trends in datasets	✘ Predict based on physical processes
✓ Predict large-scale trends	✘ Predict trends for specific forest sites
✓ Work for temperate forests	✘ Work for other forest types
✓ Work for ancient forests (at least forest since 1850)	✘ Work in other regions than the EU
	✘ Look at land-use legacy

2 Methods

2.1 Data collection

2.1.1 Understorey vegetation surveys

We used resurvey data across temperate deciduous forests in Europe from the forestREplot network. ForestREplot is a database network of vegetation plot records with understorey and overstorey community composition. Each dataset in this database is composed of multiple nonoverlapping (in space) plot records from two time points. The time interval between surveys in the 40 datasets and 1814 plots analysed here is considered sufficient to detect directional change in the herbaceous layer (a mean interval of 38 years, see De Frenne et al., 2013; Perring et al., 2018). Each dataset comes from a relatively homogeneous area in terms of climate and atmospheric nitrogen (N) deposition such that we considered all plots within a given dataset to have experienced the same macroclimatic and atmospheric N deposition conditions. *A priori,* our analysis focused on European temperate broadleaved deciduous forests and we therefore excluded plots from North America in the database, and any conifer-dominated plots. We also omitted forested plots known to be located on former agricultural land (Perring et al., 2018b, 2018a), and hence restrict our predictions to ancient forest (continuously forested since at least 1850).

We complemented the data from forestREplot with the resurvey data from the PASTFORWARD project (Maes et al., 2020). This data contains 192 vegetation plots from 19 European regions, scattered across spatial environmental gradients of atmospheric N deposition and climate conditions (mean annual temperature) within the Central-Western European temperate deciduous forest biome (Maes et al., 2020). ForestREplot and PASTFORWARD are highly compatible data, given their origin as a pooled effort to understand forest understorey changes under environmental change led by Verheyen et al. (2017). Understorey definitions among the datasets varied (Landuyt et al., 2020), but broadly applied the notion of ca. 1 m vegetation height (Gilliam, 2007). Next to complete species records of each plot, both databases hold information on mean annual temperature (MAT, °C), mean annual precipitation (MAP, mm) and atmospheric N (Ndep, kg N ha^{-1} y^{-1}) deposition (Bernhardt-Römermann et al., 2015; Maes et al., 2020; Perring et al., 2018a). In both datasets, overstorey cover data in selected regions, at the time of the initial and recent surveys were available. These tree cover percentages were recalculated using the Fischer correction method so that the total tree cover is mapped on values between 0 and 100% (Bernhardt-Römermann et al., 2015). The values of these environmental variables were used to train and test general additive models with cross-validation (see section 2.2).

The response variables of interest were understorey species richness, total Fischer-corrected understorey vegetation cover (%), proportion of woody species (%) and proportion of forest specialists (%). Richness and Fischer-corrected vegetation cover were directly estimated from the forestREplot and PASTFORWARD databases (Bernhardt-Römermann et al., 2015). The proportion of woody species (%) was estimated from the LEDA trait database, as "woodiness" is a categorical trait included in this database (Kleyer et al., 2008). We counted all woody species in a plot and calculated the proportion of woody species as the ratio of number of woody species: total richness. This proportion of woody species can be a proxy for the amount of woody regeneration in the understorey. Similarly, we included a proportion of forest specialists (woody or non-woody) from the database of Heinken et al. (2019). We use the proportion of forest specialists as a proxy to the amount of species with conservation concern, as these are the species that are specifically linked to ancient forests. Heinken et al. (2019) have created a list of vascular plant species and their affinity to forests in discrete classes. As classifications of species within this list is specific to European regions, we tallied the number of times each species was counted as a specialist (categories "1.1" and "1.2"). If this specialist tally was higher than the tally from all other classes combined, it was classified as a specialist and otherwise as a generalist. For instance, this means that e.g. *Anemone nemorosa* was entered as a generalist, although it is classed in Belgium as a specialist (Hermy et al., 1999; Verheyen et al., 2003). This is because in many parts of Northern Europe it is found in pastures (Brunet et al., 2012; De Frenne et al., 2011).

2.1.2   Setting spatial boundaries of the DSS

We specified the spatio-environmental boundaries as the Central-Western European areas with temperate or mixed deciduous forest. For this, we used the climatic stratification of Europe by Metzger et al. (2005) to identify this biome. We selected the area that is taken up by the Atlantic Central, Atlantic North, Continental, Nemoral and Pannonian Environmental Zones (Metzger et al., 2005). This selection allows for temperate deciduous broadleaved forest types, which are not included in the Boreal zones of Northern Europe, the Mediterranean zones in Southern Europe, and any high-altitude Alpine zones.

We overlaid the selected environmental zones with the Nomenclature of Territorial Units for Statistics (NUTS) administrative regions of the European Union (EU). This nomenclature of administrative boundaries allows to aggregate regional environmental data in the EU (or *a dato* 2020 affiliated to EU such as the United Kingdom and the Swiss Confederation). These administrative units are a common nomenclature that can be easily translated for intra- and supranational policies. We selected the NUTS level 1 for our purpose, which separates administrative regions of countries on the level of major socioeconomic regions (e.g. *Regions* in Belgium, *BundesLänder* in Germany, the national level in Czech

Republic). To aggregate gridded environmental data on a regional level, we randomly distributed 30 sample points within each NUTS region and falling within the overlapping extent of the temperate forest biome (Figure 1). Sample points were thus never outside our intended temperate forest environmental zone, even when a NUTS-1 region also contains another environmental zone (e.g. Alpine areas in Switzerland). These sample points were used to calculate regional averages of environmental variables (MAT, MAP, N deposition and pH) that originated from pan-European gridded data, as explained in the next section, and that are used as input to the DSS. As explained in the next section, we used similar environmental data sources for the GAM but with a focus on the area around the specific plots.
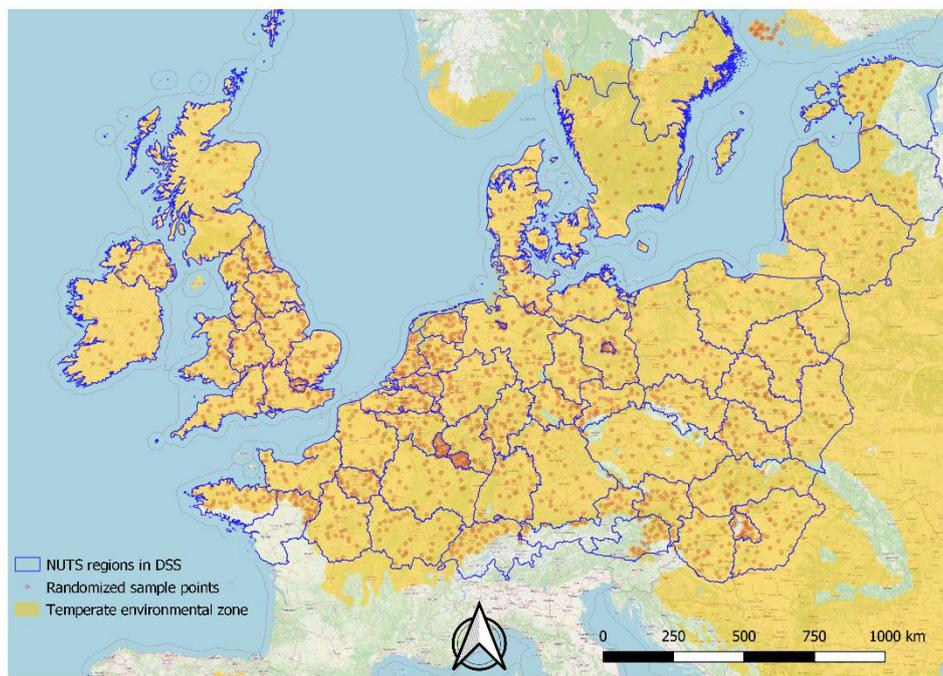
Figure 1. Extent of underSCORE in the EU, following the environmental zones of the temperate forest biome.

2.1.3 Environmental data for starting conditions of the DSS

We used the CRU TS3.4 climate database to calculate the long-term climate over the period 1980 – 2015. We recalculated this monthly data of average surface temperature ("tmp") and precipitation ("pre") into mean annual temperature (MAT) and mean annual precipitation (MAP) values and use these aggregate means as the contemporary climatic input data of the DSS. We use the long-term climate mean within this period in favor of only aggregating the latest years, because interannual climate variability is common on the short term which can muddle any long-term trends. A period of ca. 30 years is a common window to accurately estimate a long-term climate mean (Fick, 2017). Climate change has already caused an average increase in temperature of ca. 1 °C since the industrial revolution, with an expected warming of at least as 0.5°C on average globally for the period 2020 –

2050 depending on the carbon emission pathway (IPCC, 2018). Although the newest CRU 4 version with data up until 2019 has been released very recently in the summer of 2020 (Harris et al., 2020), we used the CRU TS3.4 data (1980 – 2015) because these data were applied in the compilation of the forestREplot and PASTFORWARD datasets (Bernhardt-Römermann et al., 2015; Maes et al., 2020). This means that the climatic training data for the GAM models have the same origin as the climatic input data of the tool, which allows for fewer extrapolation of predictions beyond the range of the original data.

We used the European Monitoring and Evaluation Programme on air pollution (EMEP) data to estimate N deposition across the NUTS regions in Europe. We used the most recent N deposition data available, calculated for the year 2018. Nitrogen deposition has been steadily declining in the last decade (Dirnböck et al., 2018; Verstraeten et al., 2012), hence we used the latest annual modelled deposition available. We refrained from using long-term N deposition data (i.e. cumulated over a ca. 30 year period), because such values currently do not have a clear policy implication (Dirnböck et al., 2018). However, a solid scientific basis for including such long-term cumulative N deposition to understand biodiversity change exists (Bernhardt-Römermann et al., 2015; Rowe et al., 2017). In contrast, currently, excessive amounts of N deposition are formulated as "Critical Loads" (Bobbink et al., 2015), i.e. an annual rate of N deposition when ecosystems become saturated with N leading to negative effects. These adverse effects of excessive reactive N in ecosystems include acidification and eutrophication (De Schrijver et al., 2011; Stevens, 2019), which usually drive species loss due to an increasing dominance of nitrophilous species and a concurrent limitation of other resources (e.g. water, light, other nutrients). The critical load for N deposition in temperate forests is empirically set at $10 - 20$ kg N ha^{-1} y^{-1} (Bobbink et al., 2015), where the large range in values is dictated by e.g. canopy openness (Simkin et al., 2016). To calculate an annual deposition of reactive N, we summed the available data on dry and wet oxidized and reduced N from the EMEP MSC-W model ("DDEP_OXN_m2Grid", "WDEP_OXN_m2Grid", "WDEP_RDN_m2Grid", "DDEP_OXN_m2Grid"). We recalculated the data into an average N deposition in kg N ha^{-1}y^1 at a spatial resolution of 1 degree by 1 degree, before sampling from this gridded raster using our sampling point layer (Figure 1).

Users can include information on the canopy closure (tree cover), as a proxy for light availability at the forest floor. We selected the Fischer-corrected tree cover (Bernhardt-Römermann et al., 2015) as the proxy to canopy closure (continuous values: 0% -100%). Canopy closure is strongly influenced by tree species, gap creation and forest management intensity (Pretzsch et al., 2014; Sercu et al., 2017). Management practices such as regeneration cuts or thinning remove direct competitors of future crop trees in forest stands. These interventions serve to increase growing space for these future crop trees but also bring more light to the forest floor (Hedwall et al., 2013). This increasing light availability can

alter soil microbial communities and enhance their activity, thus raising N availability (Ma et al., 2018; Ni et al., 2018). Canopy gaps also receive more wet N deposition, along with raised light availability and warmer temperatures due to the loss of the microclimate buffering canopy trees (De Frenne et al., 2019; Zellweger et al., 2020). These factors combined lead to a potential acceleration of forest understorey responses to environmental change due to light availability (Blondeel et al., 2020; De Frenne et al., 2015). From that perspective, forest managers can manipulate the input and target values for canopy closure to buffer climate change (Zellweger et al., 2020) and N deposition (Simkin et al., 2016; Verheyen et al., 2012) effects on understorey vegetation.

We included information on topsoil pH (0-5 cm) by using the 250m resolution spatial data from the [SoilGrids](#) database. Data on field-measured pH was available for PASTFORWARD (192 plots) but not for forestREplot (1814 plots). For continuity, and avoiding a discord between data sources in PASTFORWARD and ForesREPlot, we extracted the pH values from SoilGrids for all plots and used this data throughout. The data from SoilGrids was also used for the regional input data of the DSS tool, again allowing for fewer extrapolation of predictions beyond the range of the original data. All pH values are treated as static through time.

Input values can be dynamically entered via sliders for the global change variables, i.e. N deposition and MAT. Users are thus allowed to change the input value of their region if they want to tune the input conditions to a known within-region MAT or N deposition, as such aggregated regional data obviously obscures some existing within-region variability (Blondeel et al., 2019). Precipitation (MAP) and soil acidity (pH) are treated as constants within this analysis, they do not change over time and only the regional means are used (i.e. users cannot adjust them). Changing rainfall patterns in temperate Europe, in terms of mean annual precipitation, is expected to be relatively unchanging (Rollinson and Aye, 2012), while the within-year variation might change considerably due to changes in the global climate system (Jackson et al., 2015). We decided to not include pH and MAP as dynamic inputs, given that there are no real policy outputs related to these variables.

2.1.4 Environmental data for ending conditions of the DSS: scenario analysis

We used existing policy scenarios of Nitrogen deposition (the Clean Air Outlook) and climate change (MAT in shared socioeconomic pathways [SSP]) to predict understorey property change in the future. DSS predictions end at the year 2050. Our selection of scenarios was inspired by Dirnböck et al. (2018), who evaluated forest plant species trajectories under current legislation emission scenarios of N deposition (i.e. The EU Clean Air Outlook) in combination with climate change scenarios (Representative Carbon Pathways [RCP]). Dirnböck et al. (2018) found that current legislation is likely insufficient to curb forest plant species loss in the future, especially for oligotrophic species. To

account for a customization of these scenarios, e.g. in case of requiring stricter targets, we included the option to adjust an input value via dynamic sliders into a desired target.

We included two scenarios for N deposition: a business-as-usual (BAU) scenario, and a current legislation scenario. The BAU scenario simply propagates the same annual rate of N deposition in 2018 until the final modelled year of the DSS (2050). The current legislation scenario for N deposition is presented by the Clean Air Outlook of the European Commission. The Clean Air Outlook (COM(2018)446) was published in June 2018 and formulates agreed objectives on air pollution emissions from industry and agriculture. The targets of the Clean Air Outlook are available on the Greenhouse Gas – Air Pollution Interactions and Synergies portal (GAINS). We selected the European N deposition EMEP 28km SVG gridded data (available on map view under tab "Air quality and impacts"), with the scenario specified as "EU Outlook 2017 – ver Dec. 2018" and "REF_post2014_CLE_v.Dec.2018" (see also Dirnböck et al., 2018). We recalculated the unit of eq N ha^{-1}y^{-1} by applying the conversion factor of 1 keq N ha^{-1}yr^{-1} equal to 14 kg N ha^{-1}yr^{-1}. We used our set of 30 sample points per NUTS-1 region to calculate an average scenario-specific N deposition within each included region (see section 2.1.2).

We included four climate change scenarios, based on Shared Socio-economic Pathways (SSPs). The SSPs are a set of carbon emission scenarios driven by different socioeconomic assumptions for the future. These SSPs are included in the Sixth Assessment Report of the International Panel on Climate Change (IPCC AR6). The SSPs are compatible with the Representative Carbon Pathways (RCPs), formulated in the IPCC AR5 report. RCPs are scenarios that examined different possible future greenhouse gas emissions and were named after the radiative forcing (W m^{-2}) that they could engender (RCP 2.6; RCP 4.5; RCP 6.0; RCP 8.5). The updated scenarios of SSPs also translate into a radiative forcing level, that is SSP1 – 2.6; SSP2 – 4.5, SSP3 - 7.0 and SSP5 – 8.5. The SSP scenarios come with a narrative to describe the socio-economic pathway that leads to a specific emissions amount (Table 2). SSP4 was not included in the DSS, given the lack of available data for this scenario on the WorldClim database.

The data of future climate under these scenarios is available from the Coupled Model Intercomparison Project Phase 6 (CMIP, O'Neill et al., 2016). The available data are downscaled future climate projections with WorldClim v2.1 as baseline climate data. Nine models were available via WorldClim to include as a source for target MAT under the different SSPs. We selected 10 minutes gridded data of the IPSL-CM6A-LR model, as this is a European (French) model that is linked to the ORCHIDEE dynamic global vegetation model and consequently fitted for our temperate European forest focus. We selected the period of 2041 – 2060, as our ending year of 2050 nicely fits in the center of this

available climate period. We used our set of 30 sample points per NUTS-1 region to calculate an average MAT over this period for each included region and SSP scenario (see section 2.1.2).

Table 2. Narratives that are included with each of the SSP scenarios (O'Neill et al., 2017).

SSP1 **Sustainability – Taking the Green Road (Low challenges to mitigation and adaptation)**
The world shifts gradually, but pervasively, toward a more sustainable path, emphasizing more inclusive development that respects perceived environmental boundaries. Management of the global commons slowly improves, educational and health investments accelerate the demographic transition, and the emphasis on economic growth shifts toward a broader emphasis on human well-being. Driven by an increasing commitment to achieving development goals, inequality is reduced both across and within countries. Consumption is oriented toward low material growth and lower resource and energy intensity.

SSP2 **Middle of the Road (Medium challenges to mitigation and adaptation)**
The world follows a path in which social, economic, and technological trends do not shift markedly from historical patterns. Development and income growth proceeds unevenly, with some countries making relatively good progress while others fall short of expectations. Global and national institutions work toward but make slow progress in achieving sustainable development goals. Environmental systems experience degradation, although there are some improvements and overall the intensity of resource and energy use declines. Global population growth is moderate and levels off in the second half of the century. Income inequality persists or improves only slowly and challenges to reducing vulnerability to societal and environmental changes remain.

SSP3 **Regional Rivalry – A Rocky Road (High challenges to mitigation and adaptation)**
A resurgent nationalism, concerns about competitiveness and security, and regional conflicts push countries to increasingly focus on domestic or, at most, regional issues. Policies shift over time to become increasingly oriented toward national and regional security issues. Countries focus on achieving energy and food security goals within their own regions at the expense of broader-based development. Investments in education and technological development decline. Economic development is slow, consumption is material-intensive, and inequalities persist or worsen over time. Population growth is low in industrialized and high in developing countries. A low international priority for addressing environmental concerns leads to strong environmental degradation in some regions.

SSP4 **Inequality – A Road Divided (Low challenges to mitigation, high challenges to adaptation)**
Highly unequal investments in human capital, combined with increasing disparities in economic opportunity and political power, lead to increasing inequalities and stratification both across and within countries. Over time, a gap widens between an internationally-connected society that contributes to knowledge- and capital-intensive sectors of the global economy, and a fragmented collection of lower-income, poorly educated societies that work in a labor intensive, low-tech economy. Social cohesion degrades and conflict and unrest become increasingly common. Technology development is high in the high-tech economy and sectors. The globally connected energy sector diversifies, with investments in both carbon-intensive fuels like coal and unconventional oil, but also low-carbon energy sources. Environmental policies focus on local issues around middle and high income areas.

SSP5 **Fossil-fueled Development – Taking the Highway (High challenges to mitigation, low challenges to adaptation)**
This world places increasing faith in competitive markets, innovation and participatory societies to produce rapid technological progress and development of human capital as the path to sustainable development. Global markets are increasingly integrated. There are also strong investments in health, education, and institutions to enhance human and social capital. At the same time, the push for economic and social development is coupled with the exploitation of abundant fossil fuel resources and the adoption of resource and energy intensive lifestyles around the world. All these factors lead to rapid growth of the global economy, while global population peaks and declines in the 21st century. Local environmental problems like air pollution are successfully managed. There is faith in the ability to effectively manage social and ecological systems, including by geo-engineering if necessary.

2.2 Model selection and validation

2.2.1 GAM model structure

We applied general additive models (GAM) to calculate non-linear relationships between environmental variables and the understorey response variables in Rstudio version 4.0.2 (R Core Team, 2019). The separate non-linear effects in GAMs are added together for multiple environmental variables, and thus produce complex compound effects depending on the input values. Given the nature of the model structure and the training data (see section 3.3), predictions from these GAMs are interpretable as trends in average understorey property values in a given set of environmental conditions on a large regional European scale. These GAMs can thus detect deviations of an average understorey property (e.g. richness) in average environmental conditions of a region (e.g. Flanders, Belgium) in future climate change scenarios. These GAMs cannot accurately predict understorey properties in a *specific* forest site where localized land-use legacies, edaphic, microclimatic and other spatio-environmental variables can cause high variability in such understorey properties. **It is important that users bear in mind that the UnderSCORE DSS only produces projections for average understorey properties based on average regional environmental conditions in temperate Europe. Hence, the usability of the output remains operable for high-level decision-makers in the EU.**

We consistently used the same predictor variables in the GAMs for all four response variables These four response variables that users view as output are *species richness, total Fischer-corrected understorey cover (%), proportion of woody species (%)* and *proportion of forest specialists (%).* We did not transform these response variables so that residuals conformed to normality, but rather selected optimal link functions given the distribution of the data. This is a *Poisson* distribution for *richness*, given that these are count values (Oksanen et al., 2019). We adopted the *beta-distribution* for the three other response variables, because these continuous proportional values bounded from 0 to 1 can be easily characterized in this distribution (Douma and Weedon, 2019). The GAM model structure always included seven terms, of which five were environmental variables (*N deposition, MAT, Tree cover, MAP* and *pH*) and two were survey-related covariates (*Plot size* and *Survey Year*). When predicting from this GAM in the DSS, the *Plot size* is set at 100 m² and the coefficient of *Survey Year* is excluded from the estimate (but not the confidence interval, see section 4). This model structure implies a space-for-time approach: the collection of environmental gradients defines a community-environment relationship on a fixed plot size, but with growing uncertainty of estimated response variables when predicting further over time.

$$Response \sim s(N\_deposition) + s(MAT) + s(Tree\_cover) + s(MAP) + s(pH) +$$
$$s(Plot\_size) + s(Survey\_Year)$$

Equation 1. Model structure for the General Additive Models (GAMs)

2.2.2 Cross-validation of models

We evaluated the model performance on the available datasets in order to make robust predictions that are not prone to inflated errors from overfitted models. For this, we cross-validated the GAMs to select the optimal splining method and the dimension (k) of the included smoothing terms. First, we randomly split the complete dataset without empty records (n = 3733) into five equal portions using the *crossv_mc* function from the *modelr* package (Wickham, 2020). The first portion (n = 747) was set aside to use as a test dataset on the final model when the training procedure via cross-validation was finished.

On the remaining 80% of the data (n = 2986), we applied a repeated five-fold cross-validation procedure to train and test the models. In this five-fold procedure, each portion ("fold", n = 597) is once used as a testing set when the other portions combined serve as the training set (n = 2389). We evaluated the model performance by calculating the root mean squared error (*rmse*) in predictions, i.e. the standard deviation of residuals in the model predictions of the test dataset. We repeated the five-cross validation procedure on six randomized sets of five portions. This gives a total of 30 (6x5) *rmse* calculated per evaluated model. The model syntax with lowest *rmse* on average was retained for further use. Models with low *rmse* would balance the benefits of overfitting, i.e. good performance on training data but poorly generalizable to other data; and underfitting, i.e. poor performance on training data but more robustly applicable to other input values.

We applied the cross-validation in three consecutive steps for a given response variable.

Step 1: Identify the optimal penalty type for the penalized regression.
Smoothers (s) in GAM are used to define a non-linear relationship between two variables via regression splines (Perperoglou et al., 2019). These regression splines model the response *y* as separate low-degree polynomials on regular intervals of the predictor variable *x.* The penalty term prevents the smoothing spline from reaching too high order polynomials which lead to overfitting the training data. We identified whether the default penalty in the smoothing term (*s*) of the *gam* function was suited to prevent overfitting. The default is set to *thin plate regression splines* (*tp*). The strength of this penalty type is its flexibility in producing fitted curves, yet this flexibility also makes it prone to overfitting which is problematic when making predictions (Perperoglou et al., 2019). As a more "conservative" penalty type, we selected penalized cubic regression splines with shrinkage. This shrinkage allows to further reduce the effective degrees of freedom to produce less variable smoothing splines that are useful for predictions (Marra and Wood, 2011). We expected that cubic regression splines with shrinkage would produce lower *rmse* values and be more applicable for predicting across a wider range of input variables.

Step 2: Stepwise selection of the dimensions (k) in each smoother (s)

After selecting the optimal penalty type for the penalized regression, we selected the upper limit on the degrees of freedom associated within the smooth term. We iteratively varied k from 3 to 10 for each term in the model, as 3 is the lowest value possible for a non-linear fit between two variables while k ~ 10 is generally an outcome of applying the automated selection within the *gam* function (activated by setting k = -1). In general, we prefer lower values for k which would benefit the model predictions by producing lower *rmse* when presented with new data, resulting in a smoother curve with less inflection points.

Step 3: Evaluate the optimized model with newly presented data

The final step in the model validation procedure returned to the original full dataset (n = 3733). One fifth (n = 747) of this dataset was previously set aside as a test set to perform this final model validation. We re-trained the GAM models on the remaining 80% of the data (n = 2986) and used this previously unused 20% portion as a new test set. In this final step, we calculated the rmse of two models: one model where the penalty type and k values are set to default, and another where the model syntax obtained from our iterative approach is used (after step 1 and 2). This way, we could evaluate whether our final model predicts more accurately when presented with new data than a default model. When the default model would produce lower rmse values, we would select that model for use in the DSS (this was not needed). However, if our custom model performed better than the default model, we went ahead and fitted our obtained model syntax to the full dataset (n = 3733). We present the model diagnostics of the final full model only for each response variable.

3 Results

3.1 Optimizing penalty

We evaluated whether selecting a custom penalty type improved the quality of predictions, i.e. produced lower root mean squared error (*rmse*) values. Our repeated cross-validation method (see section 2.2.2) provides 30 test datasets to model these predictions errors. We *a priori* expected that selecting a stricter penalty type (cubic regression splines with shrinkage, *cs*) would produce lower prediction errors than the flexible default type (thin plate regression splines, *auto*), and hence would be more suited to use in a predictive DSS.

We found no significant difference in mean prediction error between the two penalty types of the GAMs for any of the four response variables (

Table 3). However, a closer inspection to the *rmse* value distribution across the 30 observations of each penalty type reveals some variation between training datasets (Figure 2). The distributions of *rmse* reveals lower minimum values in the *cover* and *forest specialists* response variable and fewer

outlying datasets with high rmse in the *woody ratio*. There was no visual distinction for *rmse* of both penalty types in the *richness* response variable.

Based on these observations, we decided that using cubic regression splines with shrinkage (*cs*) in the GAM terms is favorable for the UnderSCORE DSS. The shrinkage in this method has indeed reduced the amount of variability in prediction errors (*rmse*) in three of the four response variables (*cover, woody and specialists*) and not performing differently than a default setting in one response variable (*richness*).
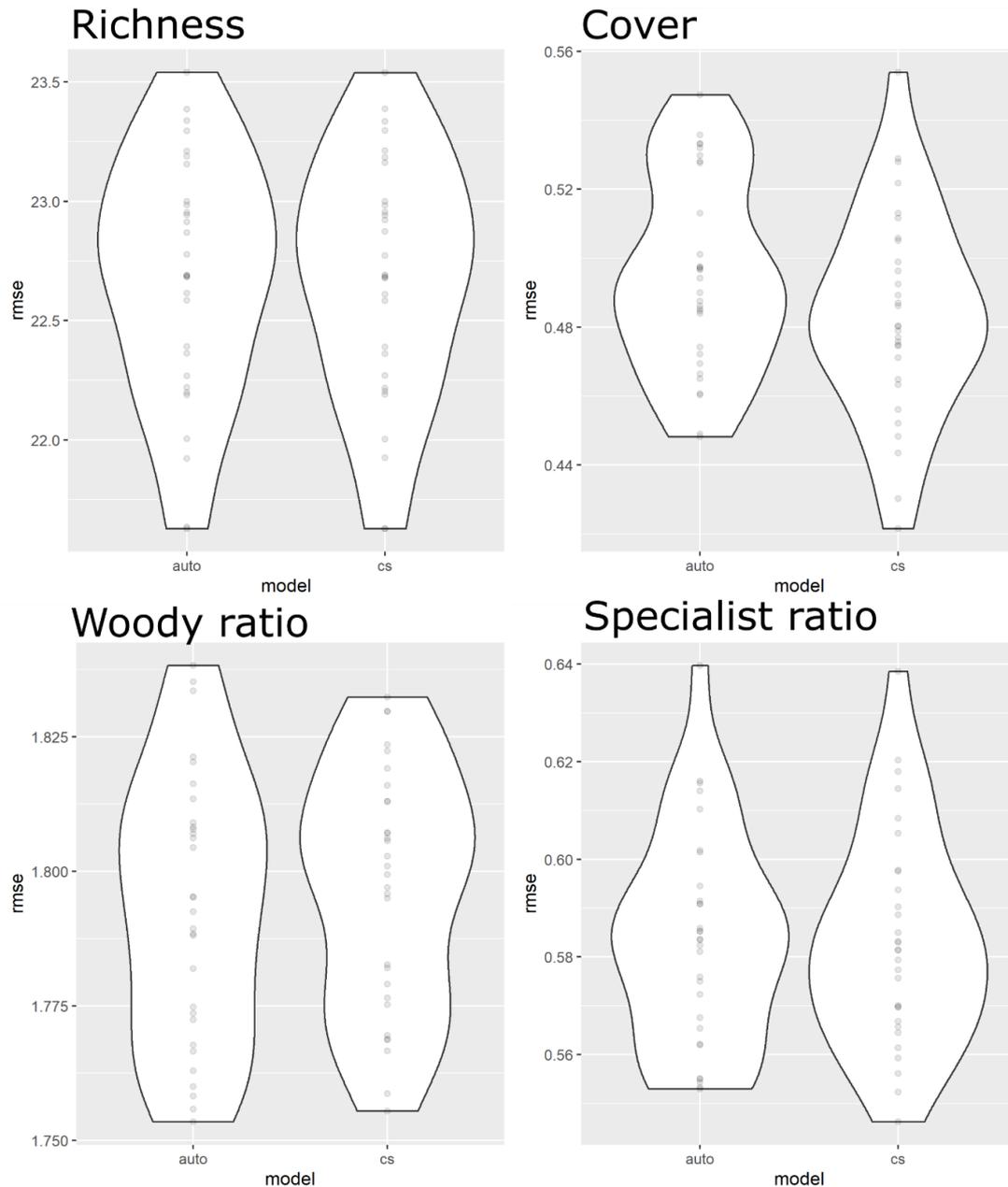
Figure 2. Distribution of root mean square errors (rmse) of model predictions using two penalty types in the training sets (n = 30).

Table 3. Estimates and standard error (S.E.) of mean prediction error (*rmse*) of the penalty in the default setting using thin plate regression splines (*Intercept*) and the estimated mean difference with the custom setting of cubic regression splines with shrinkage (*cs*). We found no significant differences in mean prediction error (rmse) between the two penalty types.

Response	Model	rmse estimate	S.E.	Chi² Statistic	P-value
Richness	(Intercept)	22.7	0.093	244	< 0.0001
Richness	cs	-0.001	0.132	-0.004	0.997
Cover	(Intercept)	0.495	0.005	93.3	< 0.0001
Cover	cs	-0.011	0.008	-1.491	0.141
Woody	(Intercept)	1.70	0.004	414	< 0.0001
Woody	cs	0.003	0.006	0.553	0.582
Specialists	(Intercept)	0.575	0.004	143	< 0.0001
Specialists	cs	0.000	0.006	-0.053	0.958

3.2   Stepwise selection of k
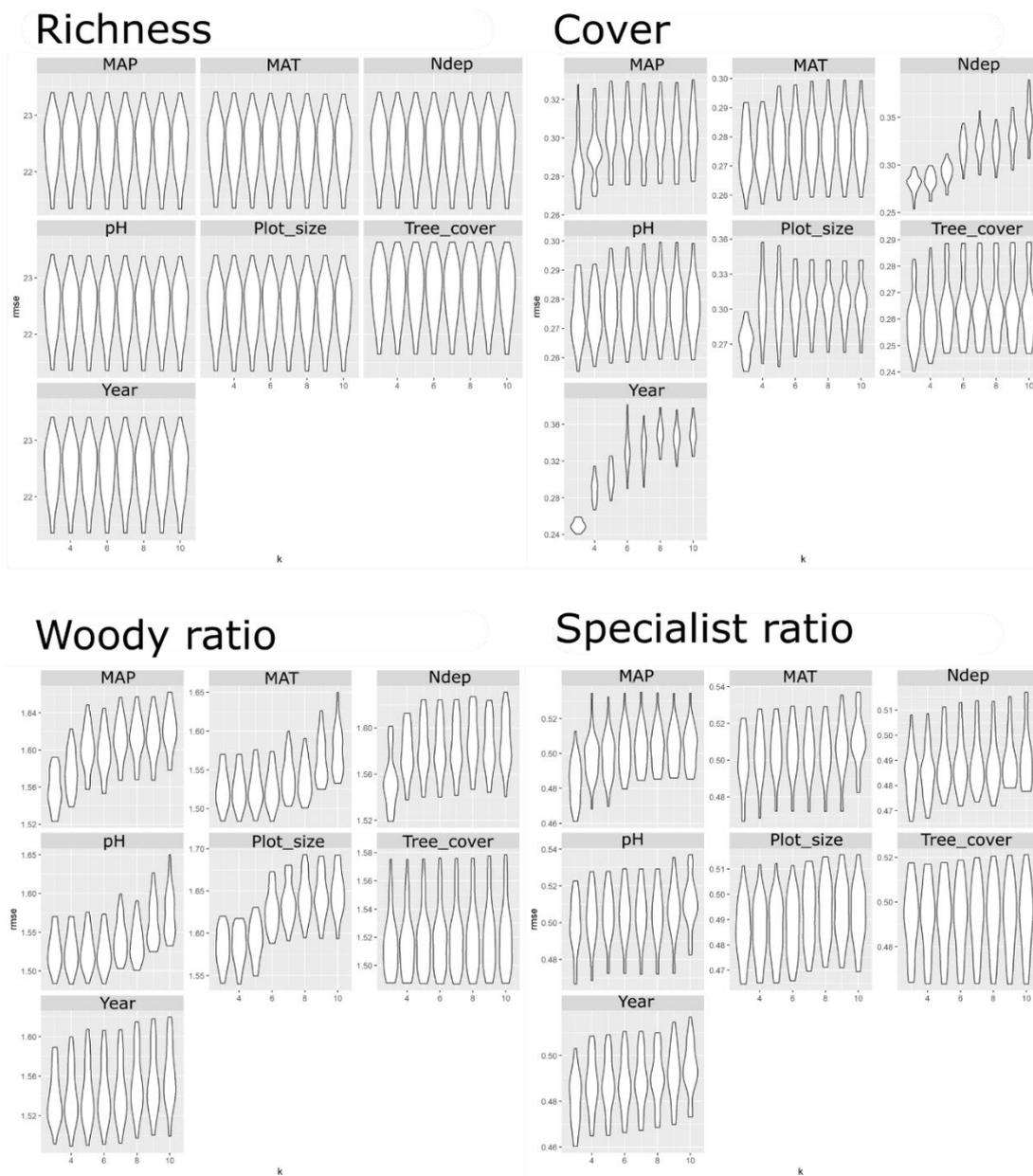
Figure 3. Stepwise selection of k (number of dimensions) in each smoothing term. Notice that lower k values generally yield lower prediction errors (*rmse*).

16

We found that low dimensions in the smoothing terms (k = 3) yielded the overall most reliable predictions by producing the lowest errors (*rmse*) when predicting from the test datasets (Figure 3). Likewise, as in optimizing the penalty, this stepwise selection of k did not provide lower predictions error in *richness* but rather showed that the smoothing terms in these GAMs were not sensitive to a change in k. For the other response variables (*cover, woody ratio* and *specialists ratio*), we found a clear separation in the distribution of prediction errors with lower *rmse* when k = 3 (Figure 3).
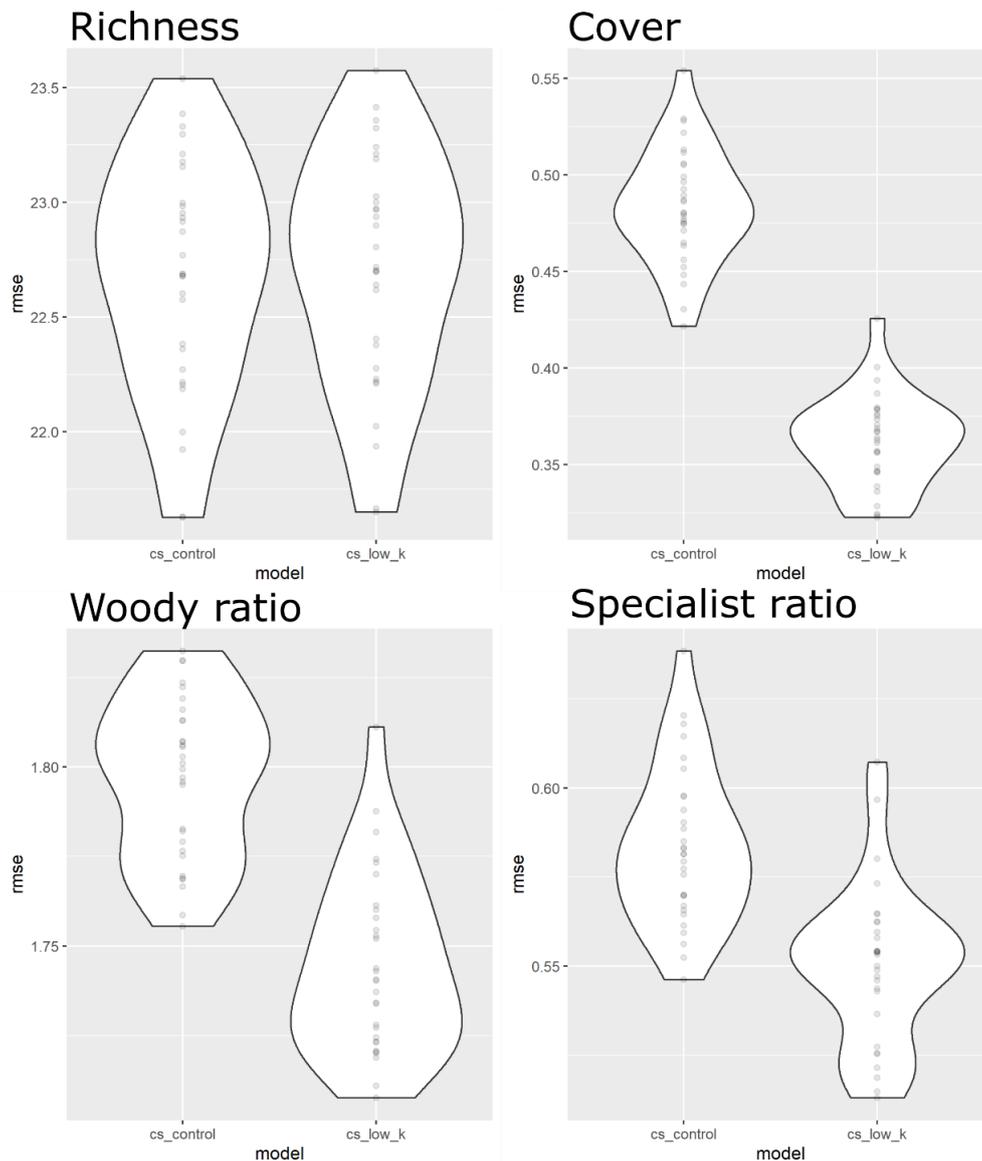
Figure 4. Distribution of root mean square errors (rmse) of model predictions from the training sets (n = 30) in the models without specifying k ("*control*") and with applying k = 3 ("*low_k*"). Both model syntaxes used cubic regression splines with shrinkage ("*cs*"), as per section 3.1.

We then compared the model prediction errors in two model syntaxes to discern whether optimizing k provides lower prediction errors. The first model syntax is a "control", where k is adjusted automatically based on the testing datasets (syntax: "k = -1") but still used cubic regression splines (see section 3.1). The other model included a fixed k value (k = 3) for all smoothing terms (see Figure

3). We found that the *rmse* was significantly (p < 0.0001) improved in three response variables (*cover, woody ratio* and *specialists*) in models with low k values (Table 4). A statistically significant lower mean prediction error when k = 3 in these three response variables is also clear when observing the whole range of *rmse* values (Figure 4). For *richness*, we again found no improvement of the prediction error with optimizing the k value, albeit no statistically distinguishable poorer performance either (Table 4). Hence, for continuity in the use of GAM, and maximizing robustness in performing predictions from these GAMs in the DSS, we used a low k value (k = 3) throughout in the final models.

Table 4. Estimates of mean prediction error (*rmse*) of the models in the default setting with internal automated selection of k (*Intercept*) and the estimated mean difference with the custom setting where k has been lowered to k = 3 (see Figure 3). P -values are highlighted in bold when this difference in *rmse* is statistically significant (alpha = 0.05).

Response	Model	rmse estimate	S.E.	Chi² Statistic	P-value
Richness	(Intercept)	22.7	0.093	243	<0.0001
Richness	cs and low k	0.025	0.132	0.190	0.849
Cover	(Intercept)	0.484	0.005	97.853	<0.0001
Cover	cs and low k	-0.122	0.007	-17.4	**<0.0001**
Woody	(Intercept)	1.80	0.004	407	<0.0001
Woody	cs and low k	-0.052	0.006	-8.36	**<0.0001**
Specialists	(Intercept)	0.583	0.004	144	<0.0001
Specialists	cs and low k	-0.033	0.006	-5.77	**<0.0001**

3.3 Performance of final model

The final model structure, after optimizing the penalty and number of dimensions (k) was equal for all the four response variables (Equation 2).

$$Response \sim s\left(N_{deposition}, bs = \text{"cs"}, k = 3\right) + s(MAT, bs = \text{"cs"}, k = 3)$$
$$+ s(Tree\_cover, bs = \text{"cs"},, k = 3)$$
$$+ s(MAP, bs = \text{"cs"}, k = 3) + s(pH, bs = \text{"cs"}, k = 3) +$$
$$s(Plot\_size, bs = \text{"cs"}, k = 3) + s(Survey\_Year, bs = \text{"cs"}, k = 3)$$

Equation 2. Final model syntax. "bs" here is the code to specifiy the penalty type, which is set to cubic regression splines with shrinkage enabled ("cs"). The k value equals 3 in all smoothing terms.

The model validation procedure returns to the full dataset (n = 3733) in the final step. One fifth (n = 747) of this dataset was initially reserved to perform this final model validation. We re-trained the GAM models on the remaining 80% of the data (n = 2986) and used this previously unused 20% portion as a final test set. In this final step, we calculated the rmse of two models: one model where the penalty type and k values are set to default, and another where the model syntax obtained from our iterative approach is used. Similarly in previous steps, we found clear separation in *rmse* for *cover, woody ratio* and *forest specialists,* which indicate better model performance by optimizing the penalty type and selection of k values in the GAM (Table 5). As before, altering the penalty type and k values

in *richness* GAMs did not change the prediction error. Hence, for our purpose, we uniformly apply cubic regression splines and a low k value (k=3) across all smoothing terms for the four response variables.

Table 5. Calculated rmse from two models trained on 80% of the data (n = 2986) and tested on an initially set-aside 20% portion of this data (n=747). Hence, this calculation is not a mean rmse but rather a single observation from this training and test dataset combination.

Response	Model	rmse
Richness	auto	22.8
Richness	cs and low k	22.8
Cover	auto	0.485
Cover	cs and low k	0.372
Woody	auto	1.81
Woody	cs and low k	1.76
Specialists	auto	0.565
Specialists	cs and low k	0.544
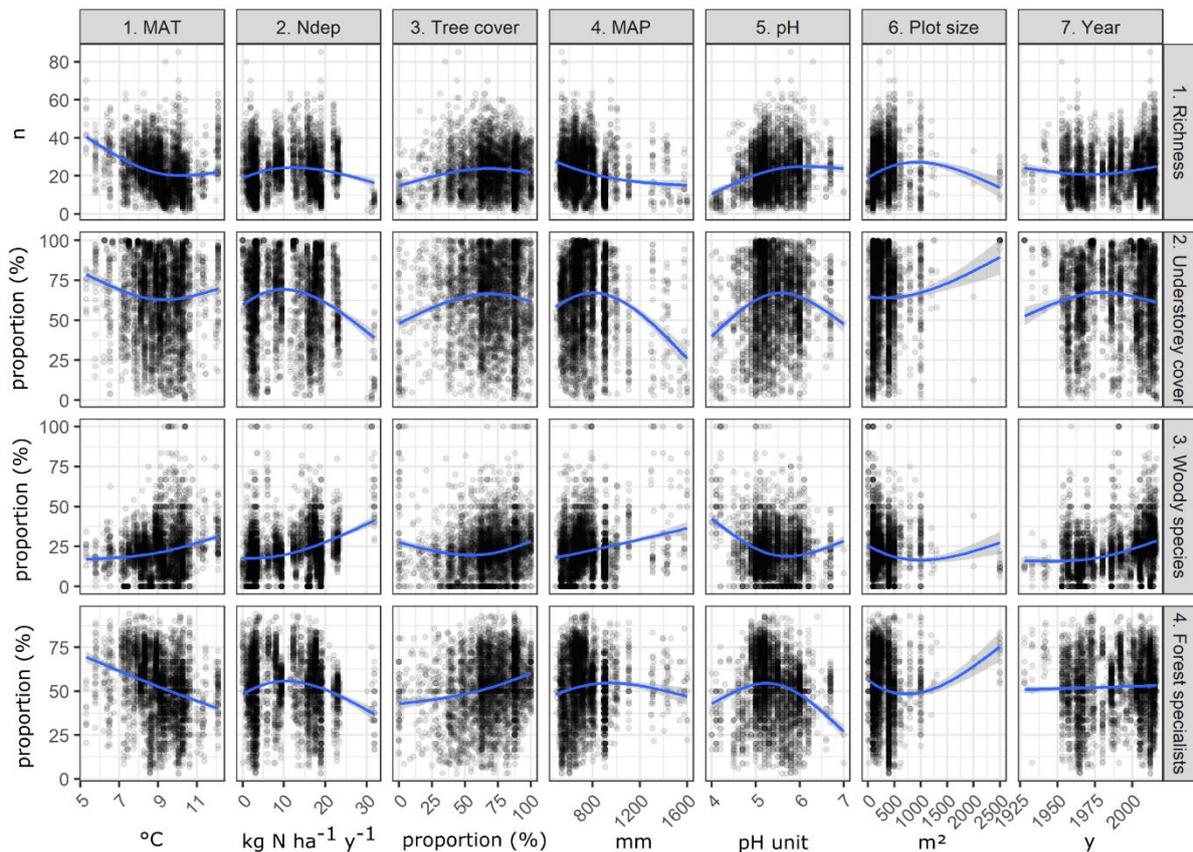
Figure 5. Two-dimensional scatterplots of the model response variables (y-axes) in response to each predictor variable (x-axes). Each smoother uses cubic regression splines with shrinkage as a penalty, with a fixed number of dimensions for the smoother (k = 3).

Pairwise scatterplots between all four response variables and each of the seven predictor variables (Figure 5) reveals considerable variation in the observations. Indeed, when reviewing the model fits for the final GAMs (Figure 6), we found relatively low R^2 overall. For richness, cover, and the proportion

of woody species, 20% of the variation was explained by the predictor variables, but with relatively even residual variance over the range of fitted values. This means that, across the range of environmental values, the mean values of observations roughly matches the mean values of predictions. However, for cover, R^2 was low (10%), which resulted in a consistent prediction of the intercept value ($0.6 - 0.7$, i.e. $60 - 70\%$ cover). Such a consistent prediction of the average cover value across the whole data range, and being insensitive to a change in environmental conditions, is a display of the poor predictive capacity of this particular model. Overall, both scatterplots (Figure 5 and Figure 6) show that the GAMs cannot accurately predict forest properties in one particular site (i.e. observation), but are capable in picking up averaged (non-linear) trends of understorey properties across environmental gradients.
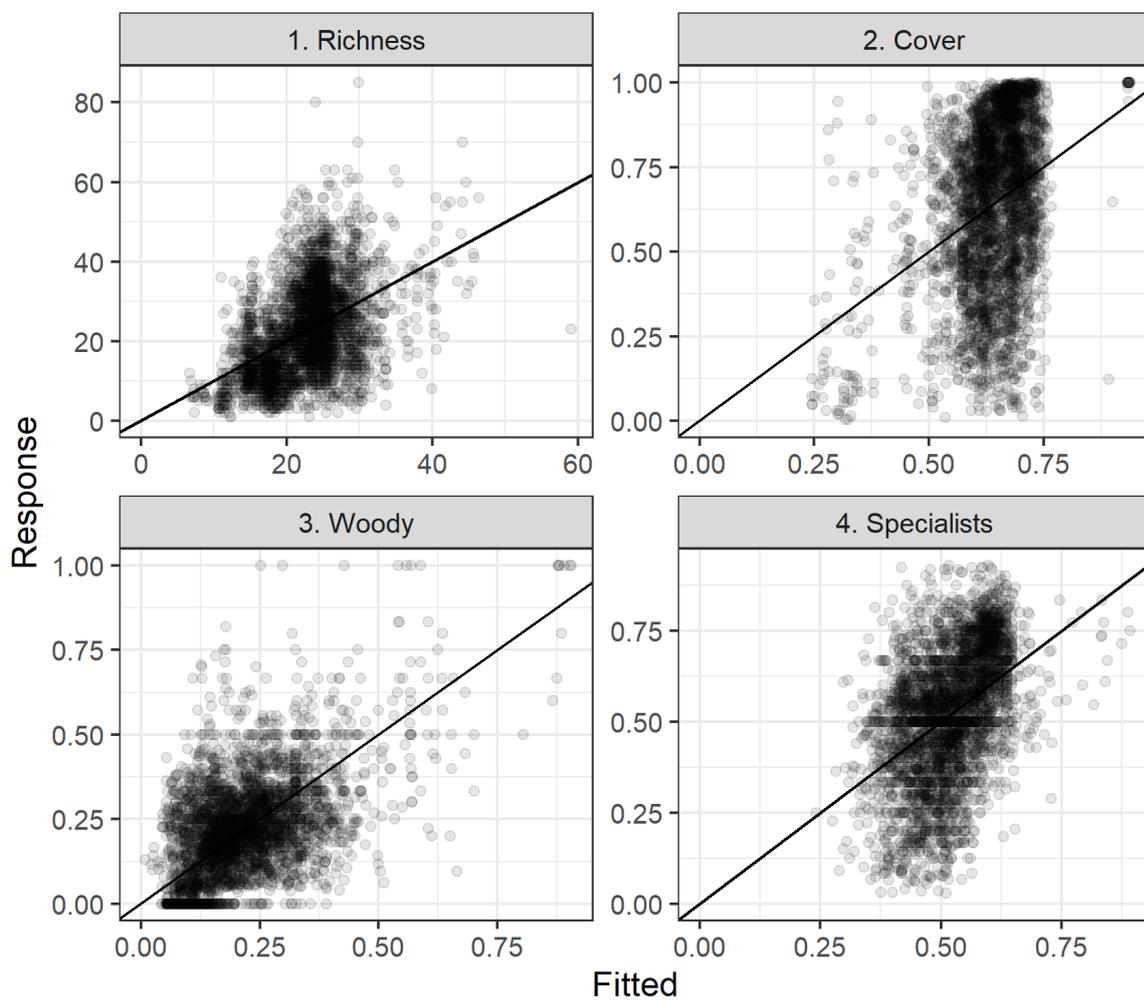
Figure 6. Model fits of each GAM for the complete dataset (n = 3733).

4 DSS at work

The underSCORE DSS is implemented with the Shiny and Leaflet libraries from R (Chang et al., 2020; Cheng et al., 2020). A specific in-depth walkthrough of the underSCORE DSS for end-users is provided in the introductory video and executive summary on the UnderSCORE web page. We present the background in the methodology of the simulation here.

The interface asks users to select a region to begin the simulation procedure (step 1). When selecting a region (e.g. Vlaams Gewest, Belgium), users will see the sliders of the input environmental conditions (conditions in 2020) change according to the average environmental values for that region (see section 2.1.3). Other metadata is also shown on a bubble in the map (Figure 7).
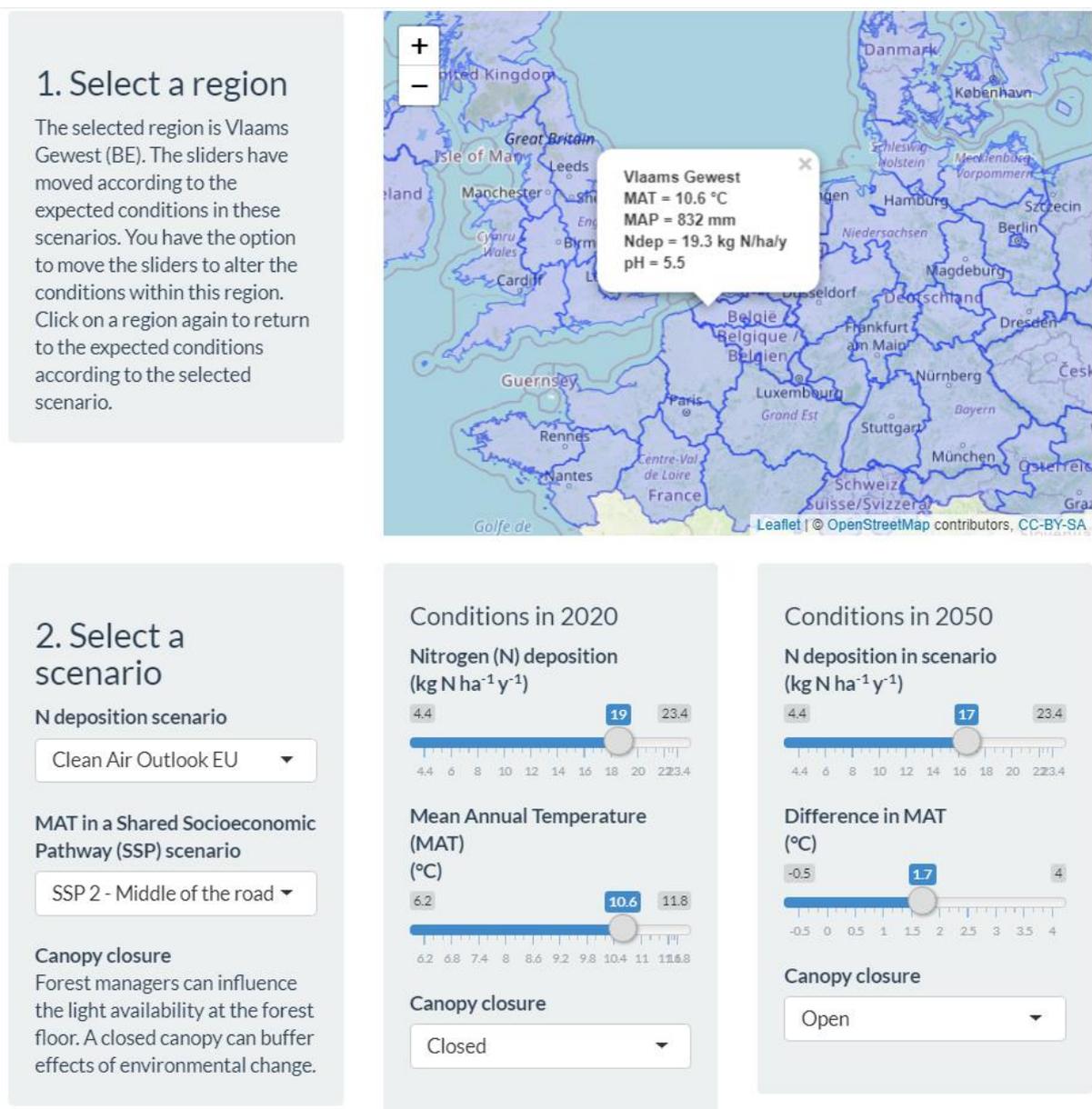
Figure 7. Excerpt from the input panel of the underSCORE DSS

Next, users can select a N deposition scenario and a climate change SSP scenario (step 2). These scenarios provide the conditions furthest removed in time, i.e. 2050 (see section 2.1.3). The difference between these environmental conditions is computed linearly over time for N deposition until the year 2030, because the Clean Air Outlook is envisioned to reach its goal by 2030. Annual N deposition in the scenario remains constant after that. In the example of Figure 7 , this means an annual decrease in N deposition of 0.2 kg N ha^{-1}y^{-1} each year for the period 2020-2030 (19 to 17 kg N ha^{-1}y^{-1} divided by ten). After that, each year has an input value of 17 kg N ha^{-1}y^{-1}. For MAT, the difference between the starting conditions and ending conditions is bridged over the whole period from 2020-2050. In the example of Figure 7, that means an annual increase of +0.057 °C (1.7°C divided by 30). Users can also select starting and ending conditions for canopy closure (i.e. tree cover). The input values correspond to open (25% cover), intermediately closed (75% cover) and closed (100% cover).

The final step displays the outputs of the DSS (Figure 8). The outputs are four simulated timeseries of the average understorey property, included 95% confidence, over the period 2020 – 2050. As explained in section 2.2.1, the predictions are performed on a fixed plot size (100 m²). The "Year" term trend is not included in the prediction of the mean values, as the model is poorly capable of coping with values larger than included in trained dataset (i.e. larger than 2015). However, Year is included in the prediction of the confidence interval. This has the favorable outcome that uncertainty of estimated response variables grows when predicting further over time.
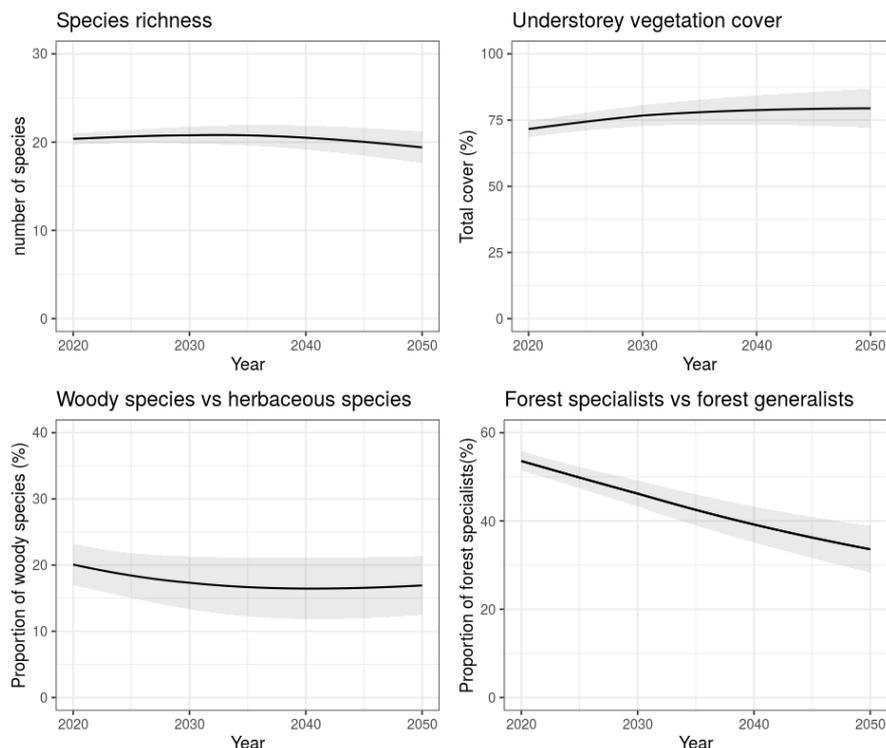
Figure 8. Output timelines of the DSS with the four response variables

5 References

Bernhardt-Römermann, M., Baeten, L., Craven, D., De Frenne, P., Hédl, R., Lenoir, J., Bert, D., Brunet, J., Chudomelová, M., Decocq, G., 2015. Drivers of temporal changes in temperate forest plant diversity vary across spatial scales. Glob. Chang. Biol. 21, 3726–3737.

Bernhardt-Römermann, M., Baeten, L., Craven, D., De Frenne, P., Hédl, R., Lenoir, J., Bert, D., Brunet, J., Chudomelová, M., Decocq, G., 2015. Drivers of temporal changes in temperate forest plant diversity vary across spatial scales. Glob. Chang. Biol. 21, 3726–3737.

Blondeel, H., Landuyt, D., Vangansbeke, P., De Frenne, P., Verheyen, K., Perring, M.P., 2021. The need for an understory decision support system for temperate deciduous forest management. For. Ecol. Manage. 480, 118634. https://doi.org/10.1016/j.foreco.2020.118634

Blondeel, H., Perring, M.P., Bergès, L., Brunet, J., Decocq, G., Depauw, L., Diekmann, M., Landuyt, D., Liira, J., Maes, S.L., Vanhellemont, M., Wulf, M., Verheyen, K., 2019. Context-dependency of agricultural legacies in temperate forest soils. Ecosystems 22, 781–795. https://doi.org/10.1007/s10021-018-0302-9

Blondeel, H., Perring, M.P., Depauw, L., De Lombaerde, E., Landuyt, D., De Frenne, P., Verheyen, K., 2020. Light and warming drive forest understorey community development in different environments. Glob. Chang. Biol. 26, 1681–1696. https://doi.org/10.1111/gcb.14955

Bobbink, R., Hicks, K., Galloway, J., Spranger, T., Alkemade, R., Ashmore, M., Bustamante, M., Cinderby, S., Davidson, E., Dentener, F., Emmett, B., Erisman, J.W., Fenn, M., Gilliam, F., Nordin, A., Pardo, L., De Vries, W., 2010. Global assessment of nitrogen deposition effects on terrestrial plant diversity: A synthesis. Ecol. Appl. 20, 30–59. https://doi.org/10.1890/08-1140.1

Bobbink, R., Tomassen, H., Weijters, M., van den Berg, L., Braun, S., Nordin, A., Schütz, K., Hettelingh, J.P., 2015. Chapter 4: Effects and empirical critical loads of Nitrogen for Europe, in: Critical Loads and Dynamic Risk Assessments. pp. 297–326. https://doi.org/10.1007/978-94-017-9508-1

Bowler, D.E., Bjorkman, A.D., Dornelas, M., Myers-Smith, I.H., Navarro, L.M., Niamir, A., Supp, S.R., Waldock, C., Winter, M., Vellend, M., Blowes, S.A., Böhning-Gaese, K., Bruelheide, H., Elahi, R., Antão, L.H., Hines, J., Isbell, F., Jones, H.P., Magurran, A.E., Cabral, J.S., Bates, A.E., 2020. Mapping human pressures on biodiversity across the planet uncovers anthropogenic threat complexes. People Nat. 2, 380–394. https://doi.org/10.1002/pan3.10071

Brunet, J., De Frenne, P., Holmström, E., Mayr, M.L., 2012. Life-history traits explain rapid colonization of young post-agricultural forests by understory herbs. For. Ecol. Manage. 278, 55–62. https://doi.org/10.1016/j.foreco.2012.05.002

Chang, W., Cheng, J., Allaire, J., Xie, Y., McPherson, J., 2020. shiny: Web Application Framework for R.

Cheng, J., Kambelkar, B., Xie, Y., 2020. leaflet: Create Interactive Web Maps with the Javascript "Leaflet."

De Frenne, P., Baeten, L., Graae, B.J., Wulf, M., Jacquemyn, H., Orczewska, A., Kolb, A., Jansen, I., Hermy, M., Diekmann, M., Schrijver, A. De, Sanctis, M. De, Decocq, G., Cousins, S.A.O., Verheyen, K., Verne, D.P.J., 2011. Interregional variation in the floristic recovery of post-agricultural forests 600–609. https://doi.org/10.1111/j.1365-2745.2010.01768.x

De Frenne, Pieter, Rodríguez-Sánchez, F., Coomes, D.A., Baeten, L., Verstraeten, G., Vellend, M., Bernhardt-Römermann, M., Brown, C.D., Brunet, J., Cornelis, J., 2013. Microclimate moderates plant responses to macroclimate warming. Proc. Natl. Acad. Sci. 110, 18561–18565.

De Frenne, P., Rodriguez-Sanchez, F., Coomes, D.A., Baeten, L., Verstraeten, G., Vellend, M., Bernhardt-Romermann, M., Brown, C.D., Brunet, J., Cornelis, J., Decocq, G.M., Dierschke, H., Eriksson, O., Gilliam, F.S., Hedl, R., Heinken, T., Hermy, M., Hommel, P., Jenkins, M.A., Kelly, D.L., Kirby, K.J., Mitchell, F.J.G., Naaf, T., Newman, M., Peterken, G., Petrik, P., Schultz, J., Sonnier, G., Van Calster, H., Waller, D.M., Walther, G.-R., White, P.S., Woods, K.D., Wulf, M., Graae, B.J., Verheyen, K., 2013. Microclimate moderates plant responses to macroclimate warming. Proc. Natl. Acad. Sci. 110, 18561–18565. https://doi.org/10.1073/pnas.1311190110

De Frenne, P., Rodríguez-Sánchez, F., De Schrijver, A., Coomes, D.A., Hermy, M., Vangansbeke, P., Verheyen, K., 2015. Light accelerates plant responses to warming. Nat. Plants 1, 1–3. https://doi.org/10.1038/nplants.2015.110

De Frenne, P., Zellweger, F., Rodríguez-Sánchez, F., Scheffers, B.R., Hylander, K., Luoto, M., Vellend, M., Verheyen, K., Lenoir, J., 2019. Global buffering of temperatures under forest canopies. Nat. Ecol. Evol. 3, 744–749. https://doi.org/10.1038/s41559-019-0842-1

De Laender, F., 2018. Community- and ecosystem-level effects of multiple environmental change drivers: Beyond null model testing. Glob. Chang. Biol. 24, 5021–5030. https://doi.org/10.1111/gcb.14382

De Schrijver, A., De Frenne, P., Ampoorter, E., van Nevel, L., Demey, A., Wuyts, K., Verheyen, K., 2011. Cumulative nitrogen input drives species loss in terrestrial ecosystems. Glob. Ecol. Biogeogr. 20, 803–816. https://doi.org/10.1111/j.1466-8238.2011.00652.x

DeMalach, N., Zaady, E., Kadmon, R., 2017. Light asymmetry explains the effect of nutrient enrichment on grassland diversity. Ecol. Lett. 20, 60–69. https://doi.org/10.1111/ele.12706

Dirnböck, T., Pröll, G., Austnes, K., Beloica, J., Beudert, B., Canullo, R., De Marco, A., Fornasier, M.F.,

Futter, M., Goergen, K., Grandin, U., Holmberg, M., Lindroos, A.J., Mirtl, M., Neirynck, J., Pecka, T., Nieminen, T.M., Nordbakken, J.F., Posch, M., Reinds, G.J., Rowe, E.C., Salemaa, M., Scheuschner, T., Starlinger, F., Uziębło, A.K., Valinia, S., Weldon, J., Wamelink, W.G.W., Forsius, M., 2018. Currently legislated decreases in nitrogen deposition will yield only limited plant species recovery in European forests. Environ. Res. Lett. 13. https://doi.org/10.1088/1748-9326/aaf26b

Douma, J.C., Weedon, J.T., 2019. Analysing continuous proportions in ecology and evolution: A practical introduction to beta and Dirichlet regression. Methods Ecol. Evol. 2019, 1412–1430. https://doi.org/10.1111/2041-210x.13234

Fick, S.E., 2017. WorldClim 2 : new 1-km spatial resolution climate surfaces for global land areas 4315, 4302–4315. https://doi.org/10.1002/joc.5086

Gilliam, F.S., 2007. The ecological significance of the herbaceous layer in temperate forest ecosystems. Bioscience 57, 845–858.

Gordon, S.N., Floris, A., Boerboom, L., Lämås, T., Eriksson, L.O., Nieuwenhuis, M., Garcia, J., Rodriguez, L., 2014. Studying the use of forest management decision support systems: an initial synthesis of lessons learned from case studies compiled using a semantic wiki. Scand. J. For. Res. 29, 44–55. https://doi.org/10.1080/02827581.2013.856463

Harris, I., Osborn, T.J., Jones, P., Lister, D., 2020. Version 4 of the CRU TS monthly high-resolution gridded multivariate climate dataset. Sci. Data 7, 1–18. https://doi.org/10.1038/s41597-020-0453-3

Hautier, Y., Niklaus, P.A., Hector, A., 2009. Competition for light causes plant biodiversity loss after eutrophication. Science (80-.). 324, 636–638. https://doi.org/10.1126/science.1169640

Hedwall, P.-O., Strengbom, J., Nordin, A., 2013. Can thinning alleviate negative effects of fertilization on boreal forest floor vegetation? For. Ecol. Manage. 310, 382–392. https://doi.org/10.1016/j.foreco.2013.08.040

Heinken, T., Diekmann, M., Liira, J., Orczewska, A., Brunet, J., Chytrý, M., Chabrerie, O., De Frenne, P., Decocq, G., Drevojan, P., Dzwonko, Z., Ewald, J., Feilberg, J., Graae, B.J., Grytnes, J.A., Hermy, M., Kriebitzch, W.-U., Laivins, M., Lindmo, S., Marage, D., Marozas, V., Meirland, A., Niemeyer, T., Paal, J., Prysek, P., Roosaluste, E., Sadlo, J., Schaminée, J.H.J., Schmidt, M., Tyler, T., Verheyen, K., Wulf, M., 2019. European forest vascular plant species list [WWW Document]. https://doi.org/https://doi.org/10.6084/m9.figshare.8095217.v1

Hermy, M., Honnay, O., Firbank, L., Grashof-Bokdam, C., Lawesson, J.E., 1999. An ecological comparison between ancient and other forest plant species of Europe, and the implications for forest conservation. Biol. Conserv. 91, 9–22. https://doi.org/10.1016/S0006-3207(99)00045-2

IPCC, 2018. Global Warming of 1.5 °C - SR15 - Summary for Policy Makers, IPCC Climate Change Synthesis Report.

Jackson, L.C., Kahana, R., Graham, T., Ringer, M.A., Woollings, T., Mecking, J. V., Wood, R.A., 2015. Global and European climate impacts of a slowdown of the AMOC in a high resolution GCM. Clim. Dyn. 45, 3299–3316. https://doi.org/10.1007/s00382-015-2540-2

Kleyer, M., Bekker, R.M., Knevel, I.C., Bakker, J.P., Thompson, K., Sonnenschein, M., Poschlod, P., Van Groenendael, J.M., Klimeš, L., Klimešová, J., Klotz, S., Rusch, G.M., Hermy, M., Adriaens, D., Boedeltje, G., Bossuyt, B., Dannemann, A., Endels, P., Götzenberger, L., Hodgson, J.G., Jackel, A.K., Kühn, I., Kunzmann, D., Ozinga, W.A., Römermann, C., Stadler, M., Schlegelmilch, J., Steendam, H.J., Tackenberg, O., Wilmann, B., Cornelissen, J.H.C., Eriksson, O., Garnier, E., Peco, B., 2008. The LEDA Traitbase: A database of life-history traits of the Northwest European flora. J. Ecol. 96, 1266–1274. https://doi.org/10.1111/j.1365-2745.2008.01430.x

Landuyt, D., De Lombaerde, E., Perring, M.P., Hertzog, L.R., Ampoorter, E., Maes, S.L., De Frenne, P., Ma, S., Proesmans, W., Blondeel, H., Sercu, B.K., Wang, B., Wasof, S., Verheyen, K., 2019. The functional role of temperate forest understorey vegetation in a changing world. Glob. Chang. Biol. 25, 3625–3641. https://doi.org/10.1111/gcb.14756

Landuyt, D., Maes, S.L., Depauw, L., Ampoorter, E., Blondeel, H., Perring, M.P., Brūmelis, G., Brunet, J., Decocq, G., den Ouden, J., Härdtle, W., Hédl, R., Heinken, T., Heinrichs, S., Jaroszewicz, B., Kirby, K.J., Kopecký, M., Máliš, F., Wulf, M., Verheyen, K., 2020. Drivers of above-ground understorey biomass and nutrient stocks in temperate deciduous forests. J. Ecol. 108, 982–997. https://doi.org/10.1111/1365-2745.13318

Landuyt, D., Perring, M.P., Seidl, R., Taubert, F., Verbeeck, H., Verheyen, K., 2018. Modelling understorey dynamics in temperate forests under global change–Challenges and perspectives. Perspect. Plant Ecol. Evol. Syst. 31, 44–54. https://doi.org/10.1016/j.ppees.2018.01.002

Ma, S., Verheyen, K., Props, R., Wasof, S., Vanhellemont, M., Boeckx, P., Boon, N., De Frenne, P., 2018. Plant and soil microbe responses to light, warming and nitrogen addition in a temperate forest. Funct. Ecol. 32, 1293–1303. https://doi.org/10.1111/1365-2435.13061

Maes, S.L., Perring, M.P., Depauw, L., Bernhardt-Römermann, M., Blondeel, H., Brūmelis, G., Brunet, J., Decocq, G., den Ouden, J., Govaert, S., Härdtle, W., Hédl, R., Heinken, T., Heinrichs, S., Hertzog, L., Jaroszewicz, B., Kirby, K., Kopecký, M., Landuyt, D., Máliš, F., Vanneste, T., Wulf, M., Verheyen, K., 2020. Plant functional trait response to environmental drivers across European temperate forest understorey communities. Plant Biol. 22, 410–424. https://doi.org/10.1111/plb.13082

Marra, G., Wood, S.N., 2011. Practical variable selection for generalized additive models. Comput.

Stat. Data Anal. 55, 2372–2387. https://doi.org/10.1016/j.csda.2011.02.004

Metzger, M.J., Bunce, R.G.H., Jongman, R.H.G., Mücher, C.A., Watkins, J.W., 2005. A climatic
stratification of the environment of Europe. Glob. Ecol. Biogeogr. 14, 549–563.
https://doi.org/10.1111/j.1466-822X.2005.00190.x

Muys, B., Hynynen, J., Palahi, M., Lexer, M.J., Fabrika, M., Pretzsch, H., Gillet, F., Briceño, E., Nabuurs,
G.-J., Kint, V., 2010. Simulation tools for decision support to adaptive forest management in
Europe. For. Syst. 3, 86. https://doi.org/10.5424/fs/201019s-9310

Ni, X., Berg, B., Yang, W., Li, H., Liao, S., Tan, B., Yue, K., Xu, Z., Zhang, L., Wu, F., 2018. Formation of
forest gaps accelerates C, N and P release from foliar litter during 4 years of decomposition in
an alpine forest. Biogeochemistry 139, 321–335. https://doi.org/10.1007/s10533-018-0474-6

O'Neill, B.C., Kriegler, E., Ebi, K.L., Kemp-Benedict, E., Riahi, K., Rothman, D.S., van Ruijven, B.J., van
Vuuren, D.P., Birkmann, J., Kok, K., Levy, M., Solecki, W., 2017. The roads ahead: Narratives for
shared socioeconomic pathways describing world futures in the 21st century. Glob. Environ.
Chang. 42, 169–180. https://doi.org/10.1016/j.gloenvcha.2015.01.004

O'Neill, B.C., Tebaldi, C., Van Vuuren, D.P., Eyring, V., Friedlingstein, P., Hurtt, G., Knutti, R., Kriegler,
E., Lamarque, J.F., Lowe, J., Meehl, G.A., Moss, R., Riahi, K., Sanderson, B.M., 2016. The
Scenario Model Intercomparison Project (ScenarioMIP) for CMIP6. Geosci. Model Dev. 9, 3461–
3482. https://doi.org/10.5194/gmd-9-3461-2016

Oksanen, J., Blanchet, G., Friendly, M., Kindt, R., Legendre, P., McGlinn, D., Minchin, P.R., O'Hara,
B.R., Simpson, G.L., Solymos, P., Stevens, M.H.H., Szoecs, E., Wagner, H., 2019. vegan:
Community Ecology Package.

Perperoglou, A., Sauerbrei, W., Abrahamowicz, M., Schmid, M., 2019. A review of spline function
procedures in R. BMC Med. Res. Methodol. 19, 1–16. https://doi.org/10.1186/s12874-019-
0666-3

Perring, M.P., Bernhardt-Römermann, M., Baeten, L., Midolo, G., Blondeel, H., Depauw, L., Landuyt,
D., Maes, S.L., De Lombaerde, E., Carón, M.M., Vellend, M., Brunet, J., Chudomelová, M.,
Decocq, G., Diekmann, M., Dirnböck, T., Dörfler, I., Durak, T., De Frenne, P., Gilliam, F.S., Hédl,
R., Heinken, T., Hommel, P., Jaroszewicz, B., Kirby, K.J., Kopecký, M., Lenoir, J., Li, D., Máliš, F.,
Mitchell, F.J.G., Naaf, T., Newman, M., Petřík, P., Reczyńska, K., Schmidt, W., Standovár, T.,
Świerkosz, K., Van Calster, H., Vild, O., Wagner, E.R., Wulf, M., Verheyen, K., 2018a. Global
environmental change effects on plant community composition trajectories depend upon
management legacies. Glob. Chang. Biol. 24, 1722–1740. https://doi.org/10.1111/gcb.14030

Perring, M.P., Diekmann, M., Midolo, G., Schellenberger Costa, D., Bernhardt-Römermann, M., Otto,
J.C.J., Gilliam, F.S., Hedwall, P.O., Nordin, A., Dirnböck, T., Simkin, S.M., Máliš, F., Blondeel, H.,

Brunet, J., Chudomelová, M., Durak, T., De Frenne, P., Hédl, R., Kopecký, M., Landuyt, D., Li, D., Manning, P., Petřík, P., Reczyńska, K., Schmidt, W., Standovár, T., Świerkosz, K., Vild, O., Waller, D.M., Verheyen, K., 2018b. Understanding context dependency in the response of forest understorey plant communities to nitrogen deposition. Environ. Pollut. 242, 1787–1799. https://doi.org/10.1016/j.envpol.2018.07.089

Pretzsch, H., Biber, P., Schütze, G., Uhl, E., Rötzer, T., 2014. Forest stand growth dynamics in Central Europe have accelerated since 1870. Nat. Commun. 5, 1–10. https://doi.org/10.1038/ncomms5967

R Core Team, 2019. R: A language and environment for statistical computing. URL https//www.r-project.org/.

Rollinson, C.H.R.R., Aye, M.A.W.K., 2012. Community assembly responses to warming and increased precipitation in an early successional forest. Ecosphere 3, 1–17.

Rowe, E.C., Jones, L., Dise, N.B., Evans, C.D., Mills, G., Hall, J., Stevens, C.J., Mitchell, R.J., Field, C., Caporn, S.J.M., Helliwell, R.C., Britton, A.J., Sutton, M.A., Payne, R.J., Vieno, M., Dore, A.J., Emmett, B.A., 2017. Metrics for evaluating the ecological benefits of decreased nitrogen deposition. Biol. Conserv. 212, 454–463. https://doi.org/10.1016/j.biocon.2016.11.022

Schmitz, A., Sanders, T.G.M., Bolte, A., Bussotti, F., Dirnböck, T., Johnson, J., Peñuelas, J., Pollastrini, M., Prescher, A.-K., Sardans, J., Verstraeten, A., de Vries, W., 2019. Responses of forest ecosystems in Europe to decreasing nitrogen deposition. Environ. Pollut. 244, 980–994. https://doi.org/10.1016/j.envpol.2018.09.101

Sercu, B.K., Baeten, L., van Coillie, F., Martel, A., Lens, L., Verheyen, K., Bonte, D., 2017. How tree species identity and diversity affect light transmittance to the understory in mature temperate forests. Ecol. Evol. 7, 10861–10870. https://doi.org/10.1002/ece3.3528

Simkin, S.M., Allen, E.B., Bowman, W.D., Clark, C.M., Belnap, J., Brooks, M.L., Cade, B.S., Collins, S.L., Geiser, L.H., Gilliam, F.S., Jovan, S.E., Pardo, L.H., Schulz, B.K., Stevens, C.J., Suding, K.N., Throop, H.L., Waller, D.M., 2016. Conditional vulnerability of plant diversity to atmospheric nitrogen deposition across the USA. Proc. Natl. Acad. Sci. U. S. A. 113, 4086–4091. https://doi.org/10.5061/dryad.7kn53

Staude, I.R., Waller, D.M., Bernhardt-Römermann, M., Bjorkman, A.D., Brunet, J., De Frenne, P., Hédl, R., Jandt, U., Lenoir, J., Máliš, F., Verheyen, K., Wulf, M., Pereira, H.M., Vangansbeke, P., Ortmann-Ajkai, A., Pielech, R., Berki, I., Chudomelová, M., Decocq, G., Dirnböck, T., Durak, T., Heinken, T., Jaroszewicz, B., Kopecký, M., Macek, M., Malicki, M., Naaf, T., Nagel, T.A., Petřík, P., Reczyńska, K., Schei, F.H., Schmidt, W., Standovár, T., Świerkosz, K., Teleki, B., Van Calster, H., Vild, O., Baeten, L., 2020. Replacements of small- by large-ranged species scale up to

diversity loss in Europe's temperate forest biome. Nat. Ecol. Evol. https://doi.org/10.1038/s41559-020-1176-8

Stevens, C.J., 2019. Nitrogen in the environment. Science (80-.). 363, 578–580.

Verheyen, K., Baeten, L., De Frenne, P., Bernhardt-Römermann, M., Brunet, J., Cornelis, J., Decocq, G., Dierschke, H., Eriksson, O., Hédl, R., Heinken, T., Hermy, M., Hommel, P., Kirby, K., Naaf, T., Peterken, G., Petřík, P., Pfadenhauer, J., Van Calster, H., Walther, G.-R., Wulf, M., Verstraeten, G., 2012. Driving factors behind the eutrophication signal in understorey plant communities of deciduous temperate forests. J. Ecol. 100, 352–365. https://doi.org/10.1111/j.1365-2745.2011.01928.x

Verheyen, K., De Frenne, P., Baeten, L., Waller, D.M., Hédl, R., Perring, M.P., Blondeel, H., Brunet, J., Chudomelová, M., Decocq, G., De Lombaerde, E., Depauw, L., Dirnböck, T., Durak, T., Eriksson, O., Gilliam, F.S., Heinken, T., Heinrichs, S., Hermy, M., Jaroszewicz, B., Jenkins, M.A., Johnson, S.E., Kirby, K.J., Kopecký, M., Landuyt, D., Lenoir, J., Li, D., Macek, M., Maes, S.L., Máliš, F., Mitchell, F.J.G., Naaf, T., Peterken, G., Petřík, P., Reczyńska, K., Rogers, D.A., Schei, F.Hø., Schmidt, W., Standovár, T., Świerkosz, K., Ujházy, K., Van Calster, H., Vellend, M., Vild, O., Woods, K., Wulf, M., Bernhardt-Römermann, M., 2017. Combining biodiversity resurveys across regions to advance global change research. Bioscience 67, 73–83. https://doi.org/10.1093/biosci/biw150

Verheyen, K., Honnay, O., Motzkin, G., Hermy, M., Foster, D.R., 2003. Response of forest plant species to land-use change: A life-history trait-based approach. J. Ecol. 91, 563–577. https://doi.org/10.1046/j.1365-2745.2003.00789.x

Verstraeten, A., Neirynck, J., Genouw, G., Cools, N., Roskams, P., Hens, M., 2012. Impact of declining atmospheric deposition on forest soil solution chemistry in Flanders, Belgium. Atmos. Environ. 62, 50–63. https://doi.org/10.1016/j.atmosenv.2012.08.017

Wickham, H., 2020. modelr: Modelling Functions that Work with the Pipe.

Zellweger, F., De Frenne, P., Lenoir, J., Vangansbeke, P., Verheyen, K., Bernhardt-Römermann, M., Baeten, L., Hédl, R., Berki, I., Brunet, J., Van Calster, H., Chudomelová, M., Decocq, G., Dirnböck, T., Durak, T., Heinken, T., Jaroszewicz, B., Kopecký, M., Máliš, F., Macek, M., Malicki, M., Naaf, T., Nagel, T.A., Ortmann-Ajkai, A., Petřík, P., Pielech, R., Reczyńska, K., Schmidt, W., Standovár, T., Świerkosz, K., Teleki, B., Vild, O., Wulf, M., Coomes, D., 2020. Forest microclimate dynamics drive plant responses to warming. Science (80-.). 368, 772–775. https://doi.org/10.1126/science.aba6880